



Research article

The potential of DEirlncRNAs: A novel approach to predict glioblastoma prognosis

Fan Yang^{a,1}, Ying Mao^{a,1}, Li Liu^a, Bo Li^{b,*}^a Department of Medical Oncology Cancer Center, Suining Central Hospital, Suining, 629000, Sichuan Province, China^b Department of Respiratory and Critical Care Medicine, Suining Central Hospital, Suining, 629000, Sichuan Province, China

ARTICLE INFO

Keywords:

Glioblastoma
DEirlncRNAs
Tumor immune infiltration
Chemotherapy

ABSTRACT

Background: Despite tremendous evolution in therapies, the prognosis of glioblastoma (GBM) remains grim, which calls for innovative approaches to optimize chemotherapy efficacy and predict risk.

Methods: The transcriptome and clinical data of GBM were acquired from the Cancer Genome Atlas (TCGA), followed by the identification of differentially expressed immune-related long noncoding RNAs (DEirlncRNAs) with Pearson correlation and limma packet analyses. Survival-related DEirlncRNA pairs were screened with univariate Cox proportional hazard regression. Prognostic markers were obtained, and risk scores were calculated with Lasso regression and multivariate Cox risk regression analyses. The association of the prognostic risk model with immune cell infiltration was evaluated by comprehensively analyzing tumor-infiltrating immune cells with TIMER, XCELL, CIBERSORT, QUANTISEQ, and EPIC. Differences in half-maximal inhibitory concentration (IC50) values between the high- and low-risk groups were assessed with the Wilcoxon signed-rank test.

Results: A total of 276 DEirlncRNAs were identified, followed by the visualization of their expression patterns. Two prognosis-related DEirlncRNA pairs were screened, with high accuracy and reliability. The constructed prognostic risk model effectively distinguished between high- and low-risk patients, and significant differences were observed in survival outcomes between the high- and low-risk groups. Furthermore, risk scores were associated with tumor-infiltrating immune cells and DEirlncRNA expression. Additionally, the risk model had a correlation with the effectiveness of commonly used chemotherapeutic agents, providing clues into potential treatment responses.

Conclusions: In our study, a novel signature was constructed with paired DEirlncRNAs (regardless of their expression), which holds significant predictive value and is a potential breakthrough for personalized management of GBM.

1. Introduction Background

Malignant gliomas, particularly glioblastoma (GBM), are the most frequent malignant primary intracranial tumors, with short

* Corresponding author. Department of Respiratory and Critical Care Medicine, Suining Central Hospital, No. 127, Desheng West Road, Chuanshan District, Suining, 629000, Sichuan Province, China.

E-mail address: libo18583081825@163.com (B. Li).

¹ They are co-first authors.

<https://doi.org/10.1016/j.heliyon.2024.e26654>

Received 17 August 2023; Received in revised form 16 December 2023; Accepted 16 February 2024

Available online 22 February 2024

2405-8440/© 2024 The Authors. Published by Elsevier Ltd. This is an open access article under the CC BY-NC-ND license (<http://creativecommons.org/licenses/by-nc-nd/4.0/>).

survival time and high recurrence, disability, and mortality rates [1]. In recent years, a Glio-DNA panel was developed based on next-generation sequencing technology, which deepens the molecular profiling of gliomas, thus providing precise data crucial for the development of personalized treatment strategies [2]. Furthermore, lactic acid was revealed to play a pivotal role in GBM progression and microenvironment alterations [3]. Additionally, a prior study demonstrated that lactic acid fostered GBM cell proliferation and migration by modulating key molecules including MCT1 and HCAR1, thereby influencing cellular phenotype and mitochondrial function [4]. These findings lay a theoretical foundation for the use of lactic acid and related molecules as promising therapeutic targets for GBM. Despite great advances in GBM treatment and the understanding of its clinicopathological and molecular characteristics, recurrent GBM has the lowest 5-year survival rates with a median survival of only 15 months [5]. Hence, further research is required to increase the therapeutic effectiveness of GBM patients.

Long non-coding RNAs (lncRNAs) are non-coding transcripts of over 200 nucleotides in length [6], which have been demonstrated to play a crucial role in cancer immunotherapy from both research and clinical perspectives ([7,8]). For instance, Zhang et al. found that lncRNA MIR22HG acted as a tumor suppressor in colorectal cancer and provided novel insight into the regulatory mechanism of the TGF β pathway, thus advancing the immunotherapy of cancers [9]. Qi et al. observed that the lncRNA SNHG14/miR-5590-3p/ZEB1 positive feedback loop facilitated the progression and immune escape of diffuse large B-cell lymphoma (DLBCL) through PD-1/PD-L1 checkpoints, illustrating SNHG14 as a potential target for improving the efficacy of immunotherapy in DLBCL patients [10]. Furthermore, Huang et al. successfully constructed a signature of irlncRNAs with strong predictive function, which provided particular guidance for analyzing the pathogenesis, clinical treatment, and potential therapeutic targets of glioma [11]. Sun et al. analyzed the expression of a set of six irlncRNAs to build a signature for predicting the survival of GBM patients [12]. Zhao et al. constructed a signature involving 5 irlncRNAs to predict the prognosis of gliomas [13]. Intriguingly, the combination of two biomarkers is more advantageous than simple genes in terms of the accuracy of a diagnostic model for cancers [14]. Nevertheless, prognostic models involving irlncRNA pairs have not been reported.

In our study, a novel modeling algorithm, pairing, and iteration were utilized to construct an irlncRNA pairs signature that did not require the specific expression of lncRNAs, followed by the evaluation of its predictive value in GBM patients, its diagnostic potency, tumor immune infiltration, and chemotherapy efficacy.

2. Methods

2.1. Data collection and differential gene analysis

The transcriptome data and clinical data of GBM were obtained from the Cancer Genome Atlas (TCGA) Data Portal (<https://tcga-data.nci.nih.gov/tcga/>). The gene transfer format file was collected from Ensembl (<http://asia.ensembl.org>) for annotation to distinguish between mRNAs and lncRNAs. Meanwhile, 2483 immune-related genes were downloaded from the ImmPort database (<http://www.immport.org>). The co-expression network of lncRNAs and immune-related genes was constructed based on the Pearson correlation coefficient to determine immune-related lncRNAs (irlncRNAs), that is, lncRNAs with an immune gene correlation coefficient greater than 0.3 and a p -value less than 0.05. Next, differentially expressed irlncRNAs (DEirlncRNAs) in the downloaded raw data were screened using the limma package, with $\log_{2}FC > 2$ and $p < 0.05$ as the screening criteria.

2.2. Construction of the prognostic signature of DEirlncRNA pairs for GBM

Stable prognostic models were extracted from the TCGA dataset, and the expression of each one was compared with that of others in the same independent sample. Next, 0-or-1 matrices were constructed through the cyclically single pairing of DEirlncRNAs by assuming $X = \text{lncRNA (Y)} - \text{lncRNA (Z)}$. In this formula, X was defined as 1 if the expression of lncRNA (Y) was higher than that of lncRNA (Z), and as 0 otherwise. Then, the constructed 0-or-1 matrices were further filtered. A match was considered valid when the number of lncRNA pairs with the expression of 0 or 1 accounted for more than 20% and less than 80% of total pairs [15]. A total of 276 DEirlncRNA pairs were attained. Univariate Cox proportional hazard regression (PHR) analyses were performed with $p < 0.01$ to screen out survival-related DEirlncRNAs pairs. The least absolute shrinkage and selection operator (Lasso) regression was performed with 10-fold cross-validation and a p -value of 0.05 for 1000 cycles, where for each cycle, the random stimulation was set at 1000 times. Thereafter, multivariate Cox PHR analyses were conducted to construct the prognostic signatures, followed by the calculation of the risk score. Furthermore, the frequency of each pair in the Lasso regression model that was repeated 1000 times was recorded, and pairs with a frequency over 100 times were used for the Cox PHR analyses and model construction. The area under the receiver-operating characteristic (ROC) curve (AUC) values for each model were calculated and plotted as curves. If the curve reached the highest point, that is, the AUC value was the maximum, the calculation was terminated, and the model was considered the optimal candidate. The 1-, 2-, and 3-year ROC curves of the model were drawn. The risk score was calculated with the following formula to build the risk model for all clinical cases: $\text{risk score} = \sum_{i=1}^k \beta_i s_i$. The maximum inflection point was determined by calculating the Akaike Information Criterion (AIC) value of each point in the 3-year ROC curve and regarded as the cutoff point to distinguish high- or low-risk scores. The cut-off value was the risk score corresponding to the minimum distance from the ROC curve to the point representing 100% true positive rate and 0% false positive rate [16]. The Kaplan–Meier curve analysis was performed with the R survival package, including “survivalROC”, “survival”, “survminer”, “glmnet”, “limma”, and “pheatmap”, was used to assess the prognostic significance of high- or low-risk scores.

2.3. Evaluation of tumor immune cell infiltration

Tumor-infiltrating immune cells in samples were comprehensively analyzed with TIMER [17], XCELL [18], CIBERSORT [19], QUANTISEQ [20], and EPIC [21] to identify the association between the prognostic risk model and immune cell infiltration. Subsequently, the Wilcoxon rank-sum test was used to analyze differences in immune-infiltrating cells analyzed by these methods between the high-risk and low-risk groups, with $p < 0.05$ as the significance parameter. The P -value was calculated with the deconvolution approach. The results were displayed in a radar chart with R package “fmsb.”

2.4. Significance of the prognostic risk model in clinical treatment

The half-maximal inhibitory concentration (IC50) of commonly used chemotherapeutic drugs in the TCGA project of the GBM dataset was calculated to evaluate the risk model in the clinical treatment of GBM. The Wilcoxon’s signed-rank test was utilized to determine the difference in IC50 between the high-risk and low-risk groups, and results were displayed as box plots obtained with “pRRophetic” and “ggplot2” of R.

3. Results

3.1. Identification of DEirIncRNA pairs

In our research, a systematic analysis was performed to ascertain the functional role of DEirIncRNA pairs in GBM and their association with immunity (Fig. 1). Initially, the TCGA database was utilized to determine lncRNA expression profiles in GBM ($n = 169$) and normal brain tissues ($n = 5$). Subsequently, 2483 genes were yielded from the ImmPort database (Table S1) and further subjected to Pearson coefficient analyses of their correlation with lncRNAs. Significantly differentially expressed lncRNAs were screened with correlation coefficient >0.3 and $P < 0.05$ as the criteria, which identified 1707 irIncRNAs (Table S2). Data normalization and differential analysis were conducted using limma, and P values were subjected to multiple-testing correction with the false discovery rate, yielding 276 DEirIncRNAs. The expression patterns of these DEirIncRNAs were visualized in a heatmap (Fig. 2a), which showed 230 upregulated DEirIncRNAs and 46 downregulated DEirIncRNAs (Table S3). In summary, our comprehensive analysis unveiled a subset of DEirIncRNAs in GBM, providing potential insights into the intricate interplay between lncRNAs and immunoregulation in the context of GBM and laying a basis for further research and development of targeted therapeutic interventions.

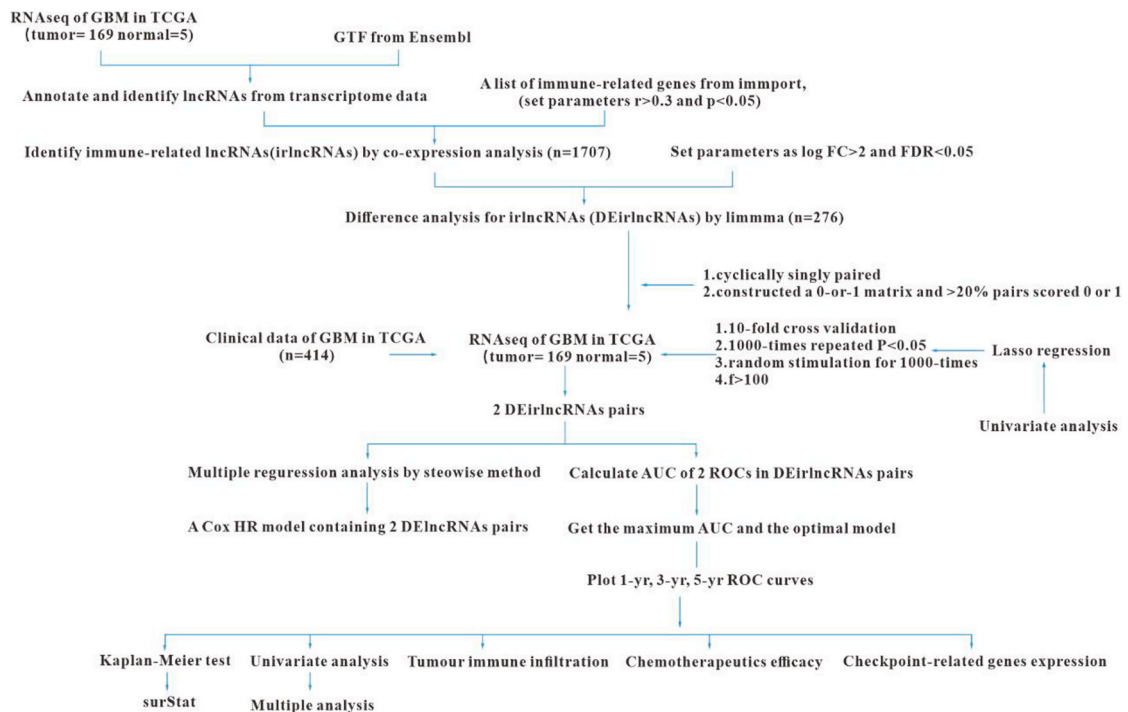


Fig. 1. The flow chart of described methods and analyses.

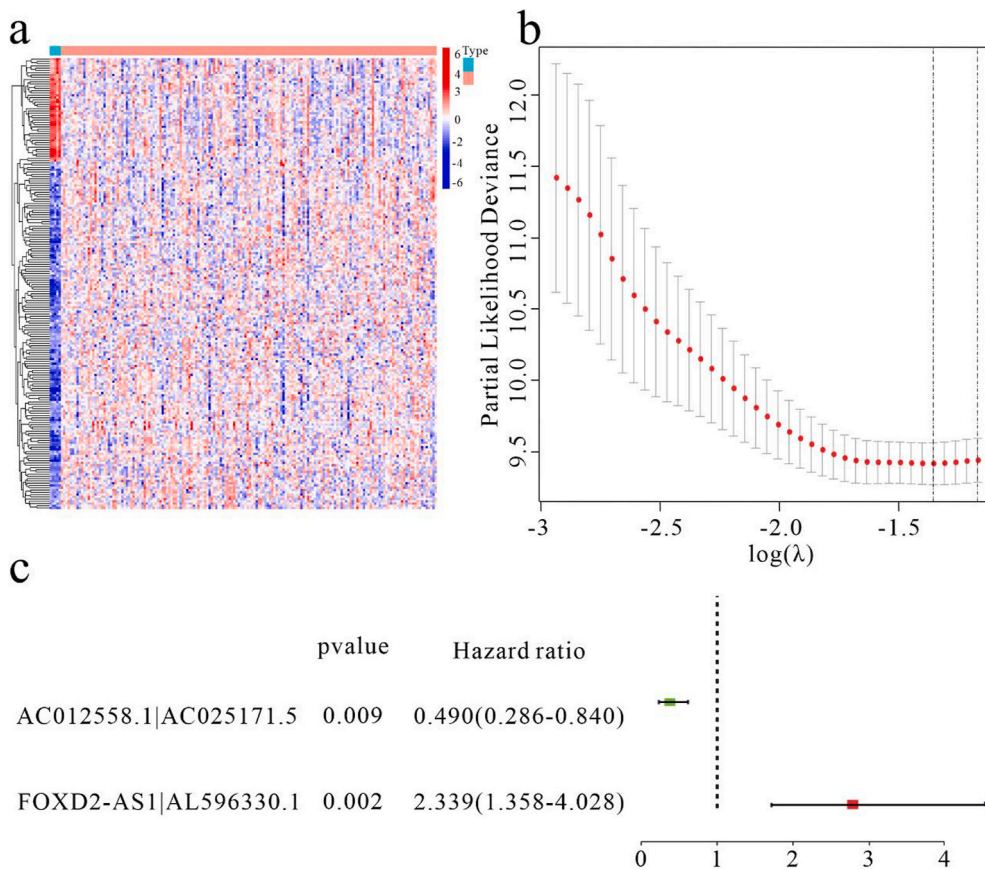


Fig. 2. Identification of DEIRlncRNAs. (a) The heatmap of the expression of DEIRlncRNAs. (b) The Lasso logistic regression model constructed with penalty parameter tuning conducted through 10-fold cross-validation based on minimum criteria. (c) A forest map showed showing 2 DEIRlncRNA pairs identified by Cox proportional hazard regression in the stepwise method.

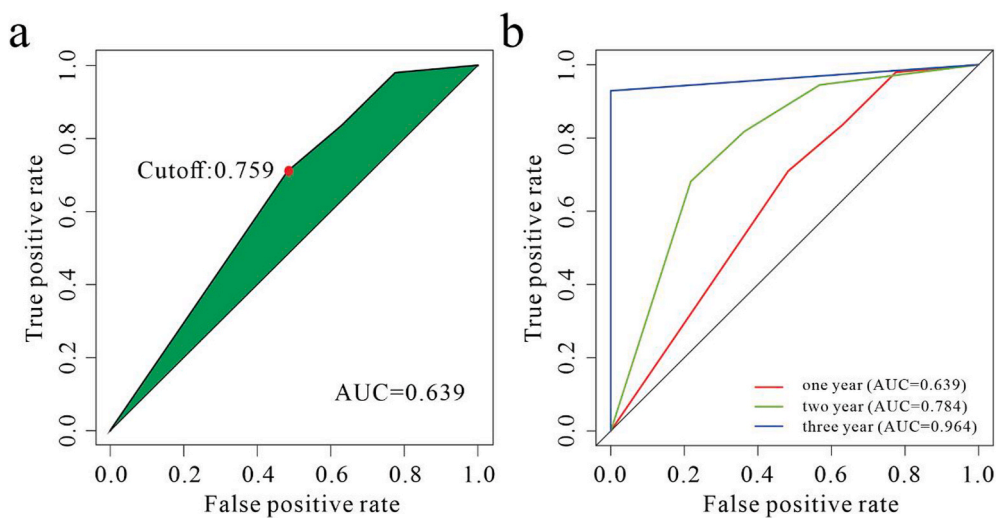


Fig. 3. A prognostic risk model of 2 DEIRlncRNA pairs. (a) A curve of every AUC value in ROC curves of the model of 2 DEIRlncRNA pairs and the highest point of the AUC. (b) ROC curves with simplified risk score to predict the 1-, 2-, and 3-year prognosis of GBM patients.

3.2. Screening of prognosis-related DEirIncRNA pairs

Subsequently, 22,743 valid DEirIncRNA pairs were successfully acquired from the DEirIncRNAs obtained above with an iterative loop and a rigorous 0-or-1 matrix screening approach (Table S4). The penalty parameters crucial for our analysis were fine-tuned through 10-fold cross-validation with the Lasso logistic regression model (Fig. 2b). After that, 2 prognosis-related DEirIncRNA pairs were obtained using a Cox proportional hazard model with the stepwise method (Fig. 2c). The prognostic accuracy of these 2 DEirIncRNA pairs was assessed by calculating AUC, which identified an optimal cutoff value of 0.759 (Fig. 3a). Notably, AUC of the 1-, 2-, and 3-year survival curves were 0.693, 0.784, and 0.964, respectively (Fig. 3b). Additionally, AIC, a measure of model fit, was calculated as 805.89. These results collectively comprehensively validated the precision and reliability of the constructed prognostic model.

3.3. Construction of a prognostic risk model with two DEirIncRNA pairs

Data of 593 GBM patients were meticulously collected from the TCGA database, followed by the calculation of individual risk scores. The cutoff value (cutoff = 0.759) was utilized to distinguish between high- and low-risk patients in the cohort for validation purposes, which categorized 88 patients into the high-risk group and 64 patients into the low-risk group (Table S5).

Further analysis exhibited markedly longer survival times in the low-risk group than in the high-risk group (Fig. 4a). This finding was further verified by Kaplan–Meier survival curves that revealed substantially lower overall survival rates in the high-risk group than in the low-risk group (Fig. 4b), substantiating the effectiveness of our risk prediction model in accurately predicting the survival and prognosis of GBM patients. In conclusion, a robust risk prediction model was constructed through comprehensive analyses of DEirIncRNA pairs to accurately predict the survival of GBM patients.

3.4. Tumor-infiltrating immune cells and DEirIncRNA expression in high- and low-risk groups

Reportedly, immune cells play dual roles as oncogenes and anti-oncogenes in tumor progression, notably in GBM [22,23]. Accordingly, the relationship between immune cells and risk scores was analyzed. The results revealed that risk scores were positively correlated with the presence of tumor-infiltrating immune cells, including T follicular helper cells (Fig. 5a) and NK cells (Fig. 5b) but negatively associated with myeloid dendritic cells (Fig. 5c), T cells CD4⁺ memory (Fig. 5d), T cells CD8⁺ (Fig. 5e), and plasmacytoid dendritic cells (Fig. 5f), as demonstrated by the Wilcoxon signed-rank test (Table S6).

Meanwhile, the relationship between DEirIncRNA expression and risk scores was also evaluated. The results unveiled that risk scores had a positive association with the expression of AC025171.5 (Fig. 6a) and FOXD2-AS1 (Fig. 6b) but a negative association with the expression of AC012558.1 (Fig. 6c) and AL596330.1 (Fig. 6d). Of note, outcomes were substantially worse in patients with high expression of AC025171.5 and FOXD2-AS1 than in patients with low expression of AC025171.5 and FOXD2-AS1 and markedly better in patients with high expression of AC012558.1 than in patients with low expression of AC012558.1 (Fig. 6e and f). The intricate relationship between immune cell infiltration and DEirIncRNA expression further underscores the potential of our risk prediction model in predicting the survival of GBM patients, which delivers valuable insights into the complex interplay between the immune microenvironment and molecular characteristics in GBM.

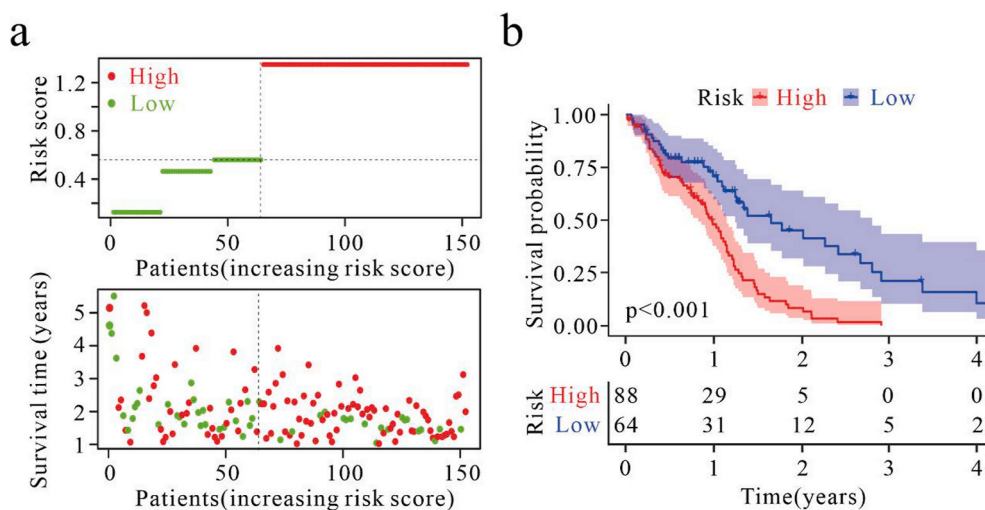


Fig. 4. Analysis of the prognostic risk score model of 2 DEirIncRNA pairs in GBM patients. (a–b) Patients in the high- and low-risk groups based on the median risk score of the prognosis risk model.

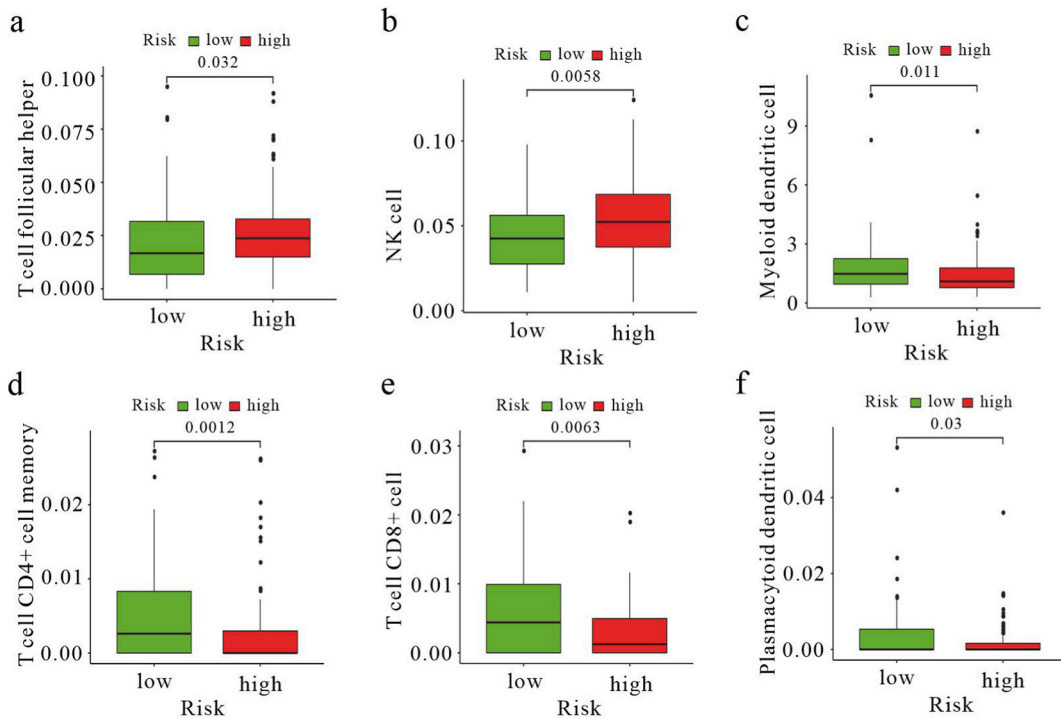


Fig. 5. Relationship between the prognostic risk score model and immune cell infiltration. (a–f) High risk was positively associated with tumor-infiltrating immune cells such as NK cells and follicular helper T cells, whereas it was negatively associated with plasmacytoid dendritic cells, myeloid dendritic cells, CD4⁺ memory T cells, and CD8⁺ T cells as demonstrated by Spearman correlation analyses.

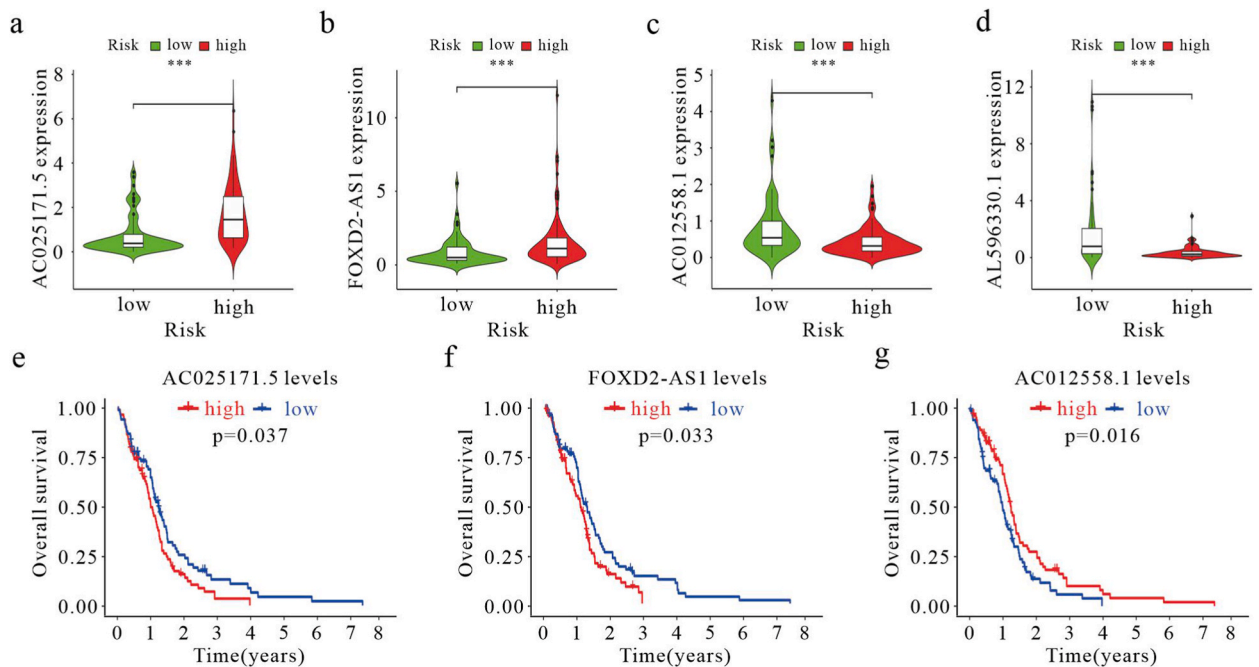


Fig. 6. Relationship between the prognostic risk score model and lincRNAs. (a–d) High-risk scores were positively correlated with upregulated AC025171.5 and FOXD2-AS1 levels, whereas they were negatively associated with the expression of AC012558.1 and AL596330.1. (e–g) Kaplan–Meier for univariate survival analysis.

3.5. Relationship between the risk model and chemotherapeutics

As the most devastating primary brain tumor, GBM is extremely resistant to traditional chemotherapy. Therefore, the current study delved into the association of risk scores with the effectiveness of common chemotherapeutic agents and immune checkpoint blockade therapy in the TCGA project for GBM. Our data unraveled that high risk scores were correlated with lower IC50 values of chemotherapeutics, including A.443654 (Fig. 7a), ABT.263 (Fig. 7b), AMG.706 (Fig. 7c), CCT007093 (Fig. 7d), KIN001.135 (Fig. 7e), OSI.906 (Fig. 7f), PF.02341066 (Fig. 7g), and SL.0101.1 (Fig. 7h). On the contrary, low risk scores were associated with lower IC50 values of chemotherapeutics (Figs. S1–2).

In conclusion, our model is expected to be a promising predictor for chemosensitivity, which can deepen the understanding of the potential efficacy of common chemotherapeutic agents in GBM treatment. Meanwhile, our findings contribute to a deeper understanding of the complex relationship between risk scores and treatment responses.

4. Discussion

GBM poses a formidable challenge due to short survival times and high recurrence and mortality rates. Because of the presence of chemoresistance, it is imperative to enhance chemotherapy efficacy and predict risk in GBM patients for improving patient outcomes ([24,25]). Nevertheless, although existing studies focus on the construction of signatures with gene expression profiles, these signatures have limited widespread applicability. Hence, innovative approaches are required.

LncRNAs, the most diverse class of non-protein-coding RNAs, participate in a wide array of molecular mechanisms regulating genome function, including intricate networks of competitive RNA-RNA interactions. For instance, LINC00483 has potential tumor-suppressive functions in colorectal cancer by regulating multiple axes [26]. Our pioneering study systematically investigated the complicated landscape of GBM and the interplay among DEirlncRNAs, risk prediction models, and treatment outcomes. In our study, a risk prediction model was constructed with DEirlncRNA pairs, with high accuracy in predicting prognosis, and obvious differences were observed in survival outcomes between the high- and low-risk groups classified with the model, emphasizing the clinical relevance and potential utility of our model.

Immune cells within the tumor microenvironment are essential for both tumor development and therapeutic responses [27–29]. Our study uncovered substantial variances in immune cell behaviors across distinct risk groups, shedding light on the tailoring of individualized treatment strategies. Elevated levels of follicular helper T cells and natural killer cells were observed in the high-risk group, consistent with existing research reporting their potential promoting functions in tumor growth and treatment resistance. Follicular helper T cells can suppress anti-tumor immune responses, whereas the dual role of natural killer cells in tumor immunity raises their functional complexity [30–32]. Our study also demonstrated higher levels of myeloid dendritic cells, CD4⁺ memory T cells, CD8⁺ T cells, and plasmacytoid dendritic cells in the low-risk group. Of note, these types of immune cells generally have positive effects on anti-tumor immunity, thus potentially mediating and amplifying anti-tumor immune responses [33–40]. More importantly, the trends of immune cells were associated with improved survival outcomes of patients in the low-risk group in our study, implicating the potential of immune cell distribution as a key indicator of underlying differences in tumor biology between the high- and low-risk groups. In this context, the type and number of immune cells are required to be carefully considered for more accurately predicting treatment responses and survival outcomes and customizing individualized treatment strategies. Nonetheless, further research and validation are warranted to elucidate the definitive mechanisms governing immune cell actions in distinct risk groups and to seamlessly incorporate this knowledge into clinical practice.

Equally groundbreaking, our model could predict chemosensitivity, thus clarifying associations between risk scores and the efficacy of common chemotherapeutic agents. Specifically, our results exhibited a correlation between high-risk scores and lower IC50 values of certain chemotherapeutics, thus offering precious information to deepen the understanding of the sophisticated network of chemoresistance in GBM. Unlike prior studies [41–43], our study focused on DEirlncRNA pairs rather than detailed expression profiles of each lncRNA, elevating the accuracy and effectiveness of the constructed model in predicting risk in GBM, which was further validated by our modified Lasso penalty model. Meanwhile, our study also probed the association of risk scores with the efficacy of common chemotherapeutic agents and immune checkpoint blockade therapy, which enhances the practicality of our findings. Overall, our signature derived from DEirlncRNA pairs (regardless of their specific expression) has excellent clinical prediction values and thus holds promise for advancing personalized treatment strategies. However, the study was performed based on TCGA data. Accordingly, this study had inherent limitations, such as sample heterogeneity and potential biases. As a result, further studies with larger and more diverse datasets are warranted to further validate our findings in the future.

Conclusively, our study not only unraveled the complexities of GBM but also introduced innovative methodologies for risk prediction and efficacy assessment. Notably, these findings not only deepen the scientific understanding of GBM but also hold enormous potential to improve the clinical outcomes of patients with this challenging disease.

5. Conclusions

In summary, our study yielded a novel risk prediction model for GBM based on DEirlncRNA pairs with high accuracy in predicting patient survival, contributing to a deeper understanding of the complex immune landscape of GBM. Additionally, our findings unraveled associations between risk scores and chemosensitivity, offering potential strategies against chemoresistance. Intriguingly, the focus of our study on DEirlncRNA pairs streamlines the predictive approach and enhances the clinical applicability of the constructed model. Altogether, our study not only advances the understanding of GBM but also yields innovative tools with practical

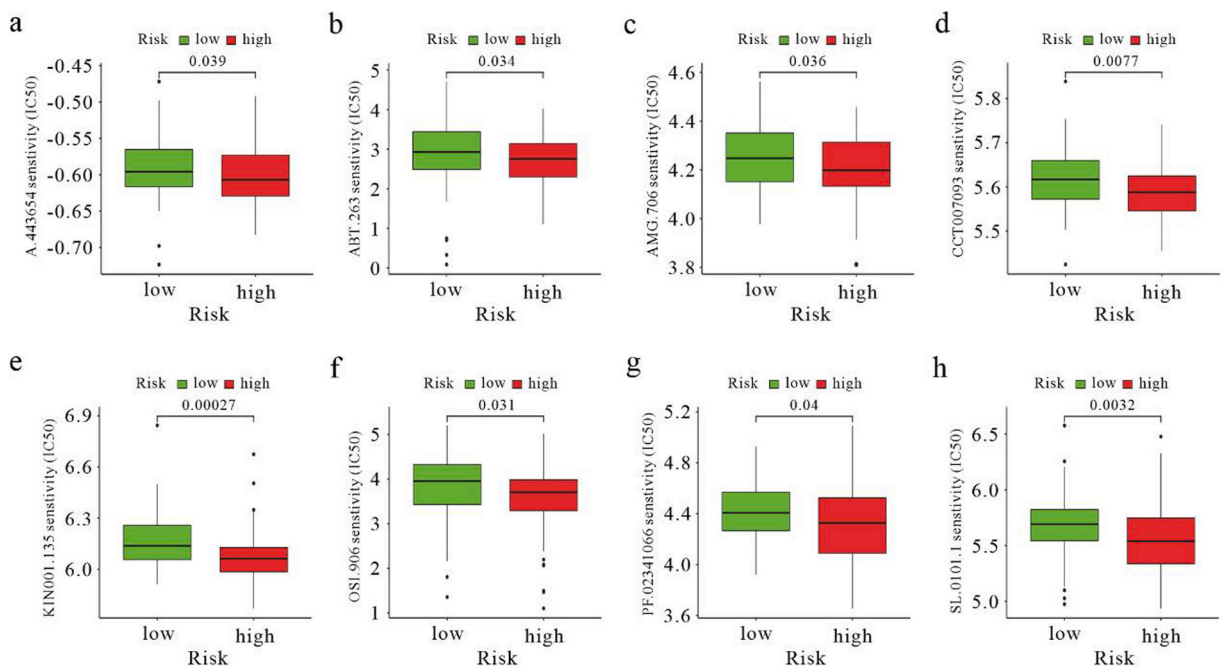


Fig. 7. The sensitivity of high-risk patients to chemotherapeutic drugs. (a–h) The model as a potential predictor for chemosensitivity as high-risk scores were related to the lower IC50 of chemotherapeutics.

implications for the development of personalized treatment strategies.

Ethics approval and consent to participate

This study protocol does not need ethics committee approval.

Consent for publication

Not applicable.

Availability of data and materials

The datasets generated and/or analyzed during the current study are available in the Cancer Genome Atlas (TCGA) Data Portal (<https://tcga-data.nci.nih.gov/tcga/>). The gene transfer format file was collected from Ensembl (<http://asia.ensembl.org>) for annotation to distinguish between mRNAs and lncRNAs. The immune-related genes were downloaded from the ImmPort database (<http://www.immport.org>).

Funding

None.

CRediT authorship contribution statement

Fan Yang: Conceptualization, Data curation, Funding acquisition, Investigation, Methodology, Project administration, Validation, Writing – original draft, Writing – review & editing. **Ying Mao:** Data curation, Funding acquisition, Investigation, Software, Writing – original draft, Writing – review & editing. **Li Liu:** Validation, Visualization, Writing – original draft, Writing – review & editing. **Bo Li:** Conceptualization, Data curation, Formal analysis, Funding acquisition, Investigation, Methodology, Project administration, Resources, Software, Supervision, Validation, Visualization, Writing – original draft, Writing – review & editing.

Declaration of competing interest

The authors declare that they have no known competing financial interests or personal relationships that could have appeared to influence the work reported in this paper.

Acknowledgments

We are very thankful to all the participants in the present research and the precious comments of Profs. We also thank the reviewers for their valuable advice.

Appendix A. Supplementary data

Supplementary data to this article can be found online at <https://doi.org/10.1016/j.heliyon.2024.e26654>.

List of abbreviations

AIC	Akaike Information Criterion
DEirlncRNAs	Differentially expressed irlncRNAs
GBM	Glioblastoma
ICIs	Immune checkpoint inhibitors
irlncRNAs	Immune-related lncRNAs
TCGA	The Cancer Genome Atlas

References

- [1] L.R. Schaff, I.K. Mellingshoff, Glioblastoma and other primary brain malignancies in adults: a review, *JAMA* 329 (2023) 574–587.
- [2] E. Tirrò, M. Massimino, G. Broggi, C. Romano, S. Minasi, et al., A custom DNA-based NGS panel for the molecular characterization of patients with diffuse gliomas: diagnostic and therapeutic applications, *Front. Oncol.* 12 (2022) 861078.
- [3] L. Longhitano, N. Vicario, S. Forte, C. Giallongo, G. Broggi, et al., Lactate modulates microglia polarization via IGFBP6 expression and remodels tumor microenvironment in glioblastoma, *Cancer Immunol. Immunother.* 72 (2023) 1–20.
- [4] L. Longhitano, N. Vicario, D. Tibullo, C. Giallongo, G. Broggi, et al., Lactate induces the expressions of MCT1 and HCAR1 to promote tumor growth and progression in glioblastoma, *Front. Oncol.* 12 (2022) 871798.
- [5] S. Mohammed, M. Dinesan, T. Ajayakumar, Survival and quality of life analysis in glioblastoma multiforme with adjuvant chemoradiotherapy: a retrospective study, *Rep Pract Oncol Radiother* 27 (2022) 1026–1036.
- [6] Z. Peng, C. Liu, MJMc Wu, New insights into long noncoding RNAs and their roles in glioma 17 (2018) 61.
- [7] Y. Li, T. Jiang, W. Zhou, J. Li, X. Li, et al., Pan-cancer characterization of immune-related lncRNAs identifies potential oncogenic biomarkers, *Nat. Commun.* 11 (2020) 1000.
- [8] J. Sun, Z. Zhang, S. Bao, C. Yan, P. Hou, et al., Identification of tumor immune infiltration-associated lncRNAs for improving prognosis and immunotherapy response of patients with non-small cell lung cancer, *Journal for immunotherapy of cancer* 8 (2020).
- [9] J. Xu, T. Shao, M. Song, Y. Xie, J. Zhou, et al., MIR22HG acts as a tumor suppressor via TGFβ/SMAD signaling and facilitates immunotherapy in colorectal cancer, *Mol. Cancer* 19 (2020) 51.
- [10] L. Zhao, Y. Liu, J. Zhang, Y. Liu, Q. Qi, lncRNA SNHG14/miR-5590-3p/ZEB1 positive feedback loop promoted diffuse large B cell lymphoma progression and immune evasion through regulating PD-1/PD-L1 checkpoint, *Cell Death Dis.* 10 (2019) 731.
- [11] P. Xia, Q. Li, G. Wu, Y. Huang, An immune-related lncRNA signature to predict survival in glioma patients, *Cell. Mol. Neurobiol.* 41 (2021) 365–375.
- [12] M. Zhou, Z. Zhang, H. Zhao, S. Bao, L. Cheng, J. Sun, An immune-related six-lncRNA signature to improve prognosis prediction of glioblastoma multiforme, *Mol. Neurobiol.* 55 (2018) 3684–3697.
- [13] X. Wang, M. Gao, J. Ye, Q. Jiang, Q. Yang, et al., An immune gene-related five-lncRNA signature for to predict glioma prognosis, *Front. Genet.* 11 (2020) 612037.
- [14] Y. Lv, S.Y. Lin, F.F. Hu, Z. Ye, Q. Zhang, et al., Landscape of cancer diagnostic biomarkers from specifically expressed genes, *Brief. Bioinform.* 21 (2020) 2175–2184.
- [15] X. Feng, S. Mu, Y. Ma, W. Wang, Development and verification of an immune-related gene pairs prognostic signature in hepatocellular carcinoma, *Front. Mol. Biosci.* 8 (2021) 715728.
- [16] B. Li, Y. Cui, M. Diehn, R. Li, Development and validation of an individualized immune prognostic signature in early-stage nonsquamous non-small cell lung cancer, *JAMA Oncol.* 3 (2017) 1529–1537.
- [17] T. Li, J. Fan, B. Wang, N. Traugh, Q. Chen, et al., TIMER: a web server for comprehensive analysis of tumor-infiltrating immune cells, *Cancer Res.* 77 (2017) e108–e110.
- [18] D. Aran, Z. Hu, A.J. Butte, xCell: digitally portraying the tissue cellular heterogeneity landscape, *Genome biology* 18 (2017) 220.
- [19] B. Chen, M.S. Khodadoust, C.L. Liu, A.M. Newman, A.A. Alizadeh, Profiling tumor infiltrating immune cells with CIBERSORT, *Methods Mol. Biol.* 1711 (2018) 243–259.
- [20] C. Plattner, F. Finotello, D. Rieder, Deconvoluting tumor-infiltrating immune cells from RNA-seq data using quanTIseq, *Methods Enzymol.* 636 (2020) 261–285.
- [21] J. Racle, D. Gfeller, EPIC: a tool to estimate the proportions of different cell types from bulk gene expression data, *Methods Mol. Biol.* 2120 (2020) 233–248.
- [22] S. Mahajan, M.H.H. Schmidt, U. Schumann, The glioma immune landscape: a double-edged sword for treatment regimens, *Cancers* 15 (2023).
- [23] Y. Li, G. Li, J. Zhang, X. Wu, X. Chen, The dual roles of human γδ T cells: anti-tumor or tumor-promoting, *Front. Immunol.* 11 (2020) 619954.
- [24] B. Huang, X. Li, Y. Li, J. Zhang, Z. Zong, H. Zhang, Current immunotherapies for glioblastoma multiforme, *Front. Immunol.* 11 (2020) 603911.
- [25] A.B. Mahmoud, R. Ajina, S. Aref, M. Darwish, M. Alsayb, et al., Advances in immunotherapy for glioblastoma multiforme, *Front. Immunol.* 13 (2022) 944452.
- [26] D. Brex, C. Barbagallo, F. Mirabella, A. Caponnetto, R. Battaglia, et al., LINC00483 has a potential tumor-suppressor role in colorectal cancer through multiple molecular axes, *Front. Oncol.* 10 (2020) 614455.
- [27] T.F. Gajewski, H. Schreiber, Y.X. Fu, Innate and adaptive immune cells in the tumor microenvironment, *Nat. Immunol.* 14 (2013) 1014–1022.
- [28] X. Lei, Y. Lei, J.K. Li, W.X. Du, R.G. Li, et al., Immune cells within the tumor microenvironment: biological functions and roles in cancer immunotherapy, *Cancer Lett.* 470 (2020) 126–133.
- [29] X. Mao, J. Xu, W. Wang, C. Liang, J. Hua, et al., Crosstalk between cancer-associated fibroblasts and immune cells in the tumor microenvironment: new findings and future perspectives, *Mol. Cancer* 20 (2021) 131.
- [30] N. Gutiérrez-Melo, D. Baumjohann, T follicular helper cells in cancer, *Trends in cancer* 9 (2023) 309–325.
- [31] A.E. Overacre-Delgoffe, H.J. Bumgarner, A.R. Cillo, A.H.P. Burr, J.T. Tometch, et al., Microbiota-specific T follicular helper cells drive tertiary lymphoid structures and anti-tumor immunity against colorectal cancer, *Immunity* 54 (2021) 2812.

- [32] Y. Yao, Z. Chen, H. Zhang, C. Chen, M. Zeng, et al., Selenium-GPX4 axis protects follicular helper T cells from ferroptosis, *Nat. Immunol.* 22 (2021) 1127–1139.
- [33] T.R. Medler, G. Kramer, S. Bambina, A.J. Gunderson, A. Alice, et al., Tumor resident memory CD8 T cells and concomitant tumor immunity develop independently of CD4 help, *Sci. Rep.* 13 (2023) 6277.
- [34] H. Pearce, W. Croft, S.M. Nicol, S. Margielewska-Davies, R. Powell, et al., Tissue-Resident memory T cells in pancreatic ductal adenocarcinoma coexpress PD-1 and TIGIT and functional inhibition is reversible by dual antibody blockade, *Cancer Immunol. Res.* 11 (2023) 435–449.
- [35] R. Reschke, J.W. Shapiro, J. Yu, S.J. Rouhani, D.J. Olson, et al., Checkpoint blockade-induced dermatitis and colitis are dominated by tissue-resident memory T cells and Th1/Tc1 cytokines, *Cancer Immunol. Res.* 10 (2022) 1167–1174.
- [36] Y. Wang, Y. Xiang, V.W. Xin, X.W. Wang, X.C. Peng, et al., Dendritic cell biology and its role in tumor immunotherapy, *J. Hematol. Oncol.* 13 (2020) 107.
- [37] A. Gardner, B. Ruffell, Dendritic cells and cancer immunity, *Trends Immunol.* 37 (2016) 855–865.
- [38] B. Reizis, Plasmacytoid dendritic cells: development, regulation, and function, *Immunity* 50 (2019) 37–50.
- [39] F. Baharom, R.A. Ramirez-Valdez, A. Khalilnezhad, S. Khalilnezhad, M. Dillon, et al., Systemic vaccination induces CD8(+) T cells and remodels the tumor microenvironment, *Cell* 185 (2022) 4317.
- [40] J. Park, P.C. Hsueh, Z. Li, P.C. Ho, Microenvironment-driven metabolic adaptations guiding CD8(+) T cell anti-tumor immunity, *Immunity* 56 (2023) 32–42.
- [41] Z.H. Feng, Y.P. Liang, J.J. Cen, H.H. Yao, H.S. Lin, et al., m6A-immune-related lncRNA prognostic signature for predicting immune landscape and prognosis of bladder cancer, *J. Transl. Med.* 20 (2022) 492.
- [42] W. Yu, Y. Ma, W. Hou, F. Wang, W. Cheng, et al., Identification of immune-related lncRNA prognostic signature and molecular subtypes for glioblastoma, *Front. Immunol.* 12 (2021) 706936.
- [43] G. Zhang, J. Sun, X. Zhang, A novel Cuproptosis-related lncRNA signature to predict prognosis in hepatocellular carcinoma, *Sci. Rep.* 12 (2022) 11325.